

## Chapter 4. Structural and thermal properties

### 4.1. Introduction

The main focus of this chapter is to study the spectroscopic, structural and thermal analysis of molecular hybrid compound based on the rare earth quinoline,  $\text{Req}_3$  ternary complexes chelated with bidentate ligand. Two bidentate ligand which are 2,2-bipyridine (Bpy) and 1,10-Phenanthroline (Phen) were coordinated as the neutral ligand (secondary ligand) to the  $\text{Req}_3$  ternary complexes. The rare earth metals that involves in the coordination are europium and terbium. Each of the analysis was performed separately in two sequential sections beginning with the europium quinolate,  $\text{Euq}_3$  ternary complexes with variations of neutral ligand and followed by Terbium quinolate, ( $\text{Tbq}_3$ ) ternary complexes with different adduction of neutral ligand. The significant differences in the characterization upon adduction of the neutral ligand were highlighted.

Both spectroscopic and structural analyses were evaluated in a thin films form. The spectroscopic study was performed by using Fourier transform infrared spectroscopy (FTIR). In this analysis, the bonding and the functional group that involves in the coordination of the metal complexes were obtained. The structural study was evaluated by using X-ray diffractometer (XRD) in order to determine the phase of the resultant molecular hybrid compounds in a thin film form. However the thermal behavior of the molecular hybrid compounds was performed in a powder form. It is worth to notice that the high durability of an organic semiconductor material is considerably important features in physical performance of organic device. It associated with the thermal stability of the organic semiconductor material. The stability and decomposition pathway of the molecular hybrid compound were investigated by thermogravimetric (TGA) and differential thermogravimetric (DTG).

## 4.2. Fourier Transform Infrared Spectroscopy (FTIR)

### 4.2.1. *Euq<sub>3</sub>bpy<sub>3</sub> and Euq<sub>3</sub>phen<sub>3</sub>*

The FTIR analysis of  $\text{Euq}_3\text{bpy}_3$  and  $\text{Euq}_3\text{phen}_3$  complexes were carried out to obtain information regarding the possible chemical bonding that is involved upon complexation of the Bpy and Phen ligands to the  $\text{Euq}_3$  ternary complexes in a thin film form. The FTIR spectra of  $\text{Euq}_3\text{bpy}_3$  and  $\text{Euq}_3\text{phen}_3$  thin films in the range of  $400.0\text{ cm}^{-1}$  to  $1800.0\text{ cm}^{-1}$  are shown in Figure 4.1. The significant vibration bands and the preliminary assignments are summarized in Table 4.1. As seen from Table 4.1, the IR spectra of the two  $\text{Euq}_3$  ternary complexes were found to be similar in spectra shape which indicates that the complexes were of similar structure. However, there were some slight shifts and intensity changes of the vibration bands detected between the two complexes that are corresponded to the different type of the neutral ligand which result in ternary complexes.

The bands at  $493.5\text{ cm}^{-1}$  and  $580.0\text{ cm}^{-1}$  of  $\text{Euq}_3\text{bpy}_3$  spectrum is assigned to the Eu-N and Eu-O bond respectively. The additions of the neutral ligand shift these bands by  $1.0\text{-}5.0\text{ cm}^{-1}$  to  $492.5$  and  $575.0\text{ cm}^{-1}$  in the  $\text{Euq}_3\text{phen}_3$  spectrum. The observed bands are in agreement with those in literature (Kumar, Srivastava, Kumar, Kamalasanan, & Singh, 2010; Luo, Chen, Tang, Xiao, & Peng, 2008; Rai et al., 2008; Thompson, Blyth, Gigli, & Cingolani, 2004; Wang, He, Liu, Shi, & Gong, 2009). It should be noted that the intermolecular metal ion bonding of the complexes were exhibited at smaller wavenumbers due to the greater mass of the europium ion ( $\text{Eu}^{3+}$ ) that is attached to the nitrogen and oxygen atoms. These results are evidence for the presence of the coordination bond between the  $\text{Eu}^{3+}$  as the metal centre of the complex and the oxygen atom from the OH (hydroxyl) group and the nitrogen atom from NH (amine) group.

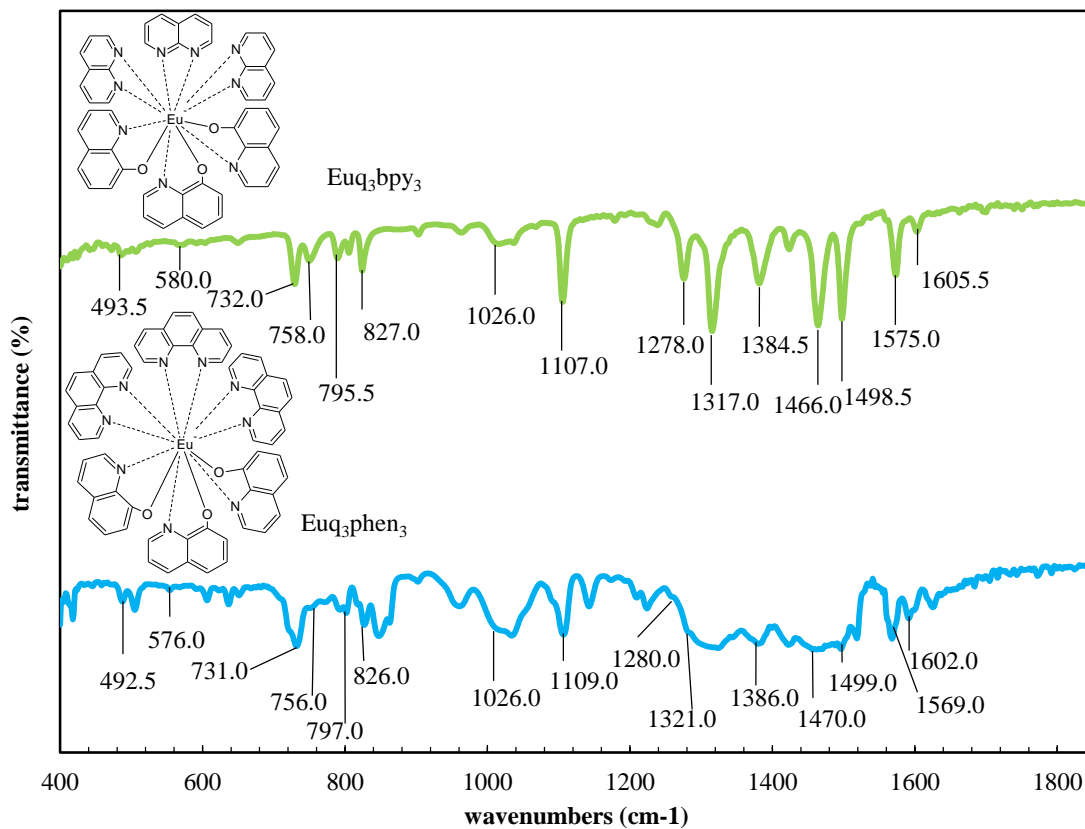


Figure 4.1 FTIR spectra of  $\text{Euq}_3\text{bpy}_3$  and  $\text{Euq}_3\text{phen}_3$  thin films range from 400- 1800  $\text{cm}^{-1}$

Table 4,1 Assignments for the vibrational spectra of Figure 4.1

Assignment	Wavenumber ( $\pm 0.1 \text{ cm}^{-1}$ )	
	$\text{Euq}_3\text{bpy}$	$\text{Euq}_3\text{phen}_3$
Eu-N	493.5	492.5
Eu-O	580.0	576.0
Aromatic ring	732.0	731.5
	758.0	756.0
	795.5	794.0
	827.0	826.5
C-N	1278.0	1280.0
	1317.0	1321.0
	1384.5	1386.5
C=C	1466.0	1470.0
C-H	1026.0	1026.0
C=N	1605.5	1602.0
C-O	1575.0	1569.0
	1107.0	1108.0
	1498.5	1499.0

The multiple absorption bands which occur at 731.0 -797.0  $\text{cm}^{-1}$  in the spectra are the characteristic of the aromatic ring. The presence of this aromatic ring is related to the existence of the 8Hq ligand that correspond to the pyridine and phenyl groups of the  $\text{Euq}_3$  ternary complexes and derivatives (Kumar, et al., 2010). The bands located within the range of 1278.0- 1280.0  $\text{cm}^{-1}$  and 1317.0-1321.0  $\text{cm}^{-1}$  in the spectra should correspond to the C-N bond that associated with the pyridine groups in the  $\text{Euq}_3$  ternary complexes and derivatives (Kumar, et al., 2010; Rai, et al., 2008). The three broad bands centered at 1470.0 and 1466.0  $\text{cm}^{-1}$  are assigned to the C=C bond while the other three intense bands located at 1026.0 and 1026.5  $\text{cm}^{-1}$  are ascribed to the C-H bond of the aromatic ring that are correlated to the 8Hq, Bpy and Phen ligands. It also should be noticed that a broad peak observe at C-H band. This is because the energy that require to stretch the hydrogen atom is less compared to the other atom.

The existence of the C-O bond in the region of 1107.0 to 1108.0 and 1498.5-1499.0  $\text{cm}^{-1}$  is referring to the possible coordination of  $\text{Eu}^{3+}$  ion to the 8Hq ligand via participation of the oxygen atom of the phenyl group. The presence of C=N bond at 1569.0, 1575.0, 1602.0 and 1605.5  $\text{cm}^{-1}$  in the spectra were found to be a good evidence for the contribution of the nitrogen atom in the complexes formation (Rai, et al., 2008). Through the FTIR spectroscopy, it can be seen that the thin films intensity of these bands appeared to be strong upon the coordination of the neutral ligand. This can be understood as, upon the coordination of the neutral ligand, the number of the nitrogen atom attached to the complexes is increased, thereby enhanced the electronegativity value of the complexes and as well as the bond dipole which consequently will result an intense absorption band.

#### 4.2.2. *Tbq<sub>3</sub>bpy<sub>3</sub> and Tbq<sub>3</sub>phen<sub>3</sub>*

The FTIR analysis of *Tbq<sub>3</sub>bpy<sub>3</sub>* and *Tbq<sub>3</sub>phen<sub>3</sub>* thin films are shown in Figure 4.2. The spectra were scan from 400.0  $\text{cm}^{-1}$  to 1800.0  $\text{cm}^{-1}$  in order to study the possible participation of the various chemical bonding that were involved upon complexation of the bpy and phen ligands to the *Tbq<sub>3</sub>* ternary complexes in a thin film form. The important IR characteristic absorption bands of the two *Tbq<sub>3</sub>* ternary complexes together with their proposed assignments are tabulated in Table 4.2. The FTIR spectra were found to exhibit an identical feature to each other except for some slight shift and intensity changes detected suggesting a similar structure among the *Tbq<sub>3</sub>* ternary complexes.

The bands located at 499.0 and 497.0  $\text{cm}^{-1}$  in the spectra are ascribed to the Tb-N bond, while the bands at 578.0 and 564.0  $\text{cm}^{-1}$  are assigned to the Tb-O bond (Xiao, Luo, Chen, Li, & Tang, 2008; Zhang, Pan, Jia, Liu, & Xu, 2012). The intermolecular bonding of metal ion was found to exhibit at the smaller wavenumber due to the heavy metal  $\text{Tb}^{3+}$  that coordinate to the nitrogen and oxygen atom. This phenomenon can be explained from the Hooke's Law which approximates the bonding vibrations are dependence to the atomic mass. Based on this law, atom with greater mass is expected to vibrate at lower frequencies. Due to this reason, the intermolecular bonding of metal ion was expected to exhibit at a smaller wavenumber, as the mass of the atoms increases, the vibration frequency decreases. These features also confirm the coordination of the Terbium ion ( $\text{Tb}^{3+}$ ) to the ligand via involvement of nitrogen atom from pyridine group and oxygen of phenyl group. The multiple absorption bands which occur in the range of 735.0-736.0 $\text{cm}^{-1}$ , 797.0-802.0 and 834.0-835.0  $\text{cm}^{-1}$  in the spectra are assigned to the aromatic ring that are associated with the pyridine and phenyl group

which are involved in the formation of the 8Hq ligand in the  $Tbq_3$  ternary complexes (Kumar, et al., 2010).

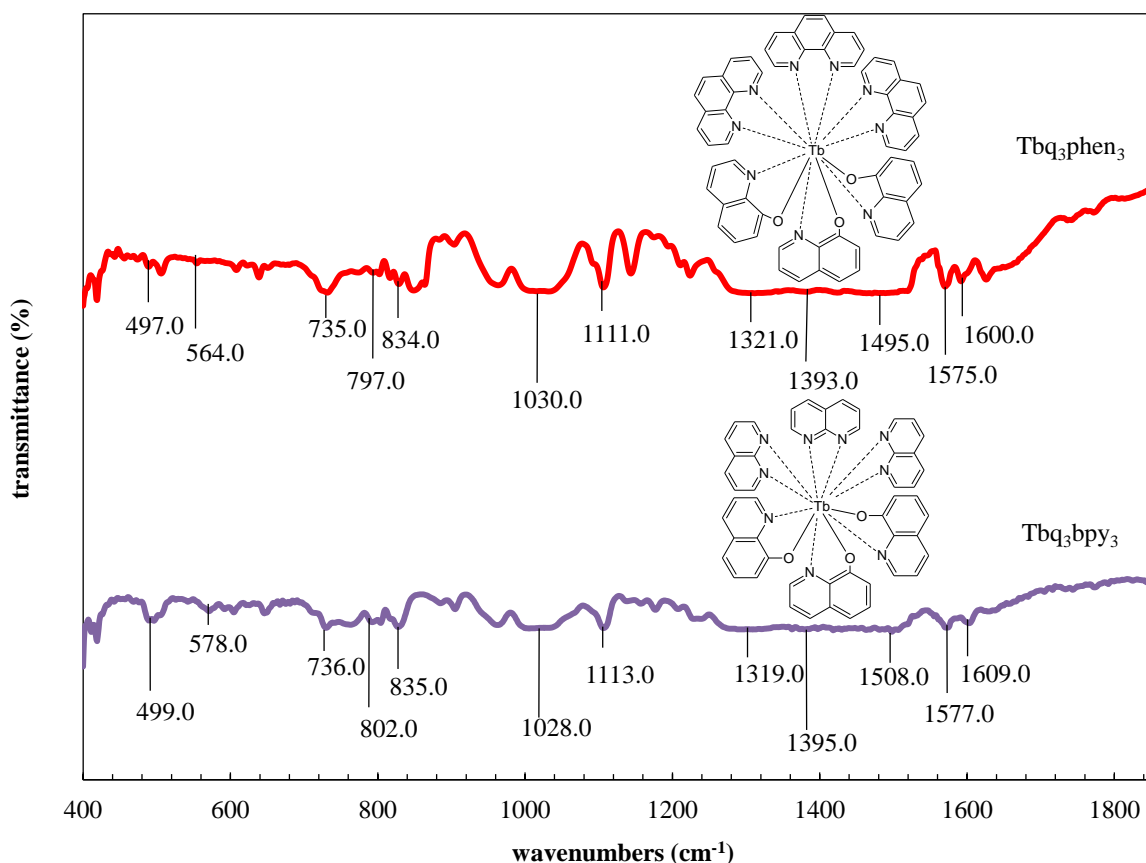


Figure 4.2 FTIR spectra of  $Tbq_3bpy_3$  and  $Tbq_3phen_3$  thin films range from 400- 1800  $cm^{-1}$

It is noteworthy that a weak absorption band that was observed in the region of 1319.0-1395.0  $cm^{-1}$  in the spectra is associated to C-N while the band located in the range of 1493.0-1508.0  $cm^{-1}$  is referring to the C=C bond. These results provide an evidence for contribution of the C=C and C-N bonds that are originated from the pyridine group of the 8Hq, Bpy and Phen ligand in  $Tbq_3$  ternary complexes. The weak intensity exhibits by these bands might be due to smaller electronegativity value of the atom that will result in less photon absorption. On the other hand, two absorption bands that are exhibited at 1028.0 and 1030.0  $cm^{-1}$  correspond to the C-H bond. The absorption band appears to be broader since less energy is required to stretch the hydrogen bond that is

attached to the carbon atom. The existence of the C-O bond at 1111.0 and 1113.0  $\text{cm}^{-1}$  is referred to the possible coordination of  $\text{Tb}^{3+}$  ion to the 8Hq ligand via participation of the oxygen atom of the phenyl group. The presence of C=N bond at 1575.0, 1577.0, 1600.0 and 1609.0  $\text{cm}^{-1}$  in the spectra were found to be a good evidence for the contribution of the nitrogen atom in the complexes formation (Rai, et al., 2008). Through the FTIR spectroscopy, it can be seen that the thin films exhibits almost the same characteristics with only minimal remarkable changes in the intensities.

**Table 4.2 Assignments for the vibrational spectra of Figure 4.2**

Assignment	Wavenumber ( $\pm 0.1 \text{ cm}^{-1}$ )	
	Tbq <sub>3</sub> bpy <sub>3</sub>	Tbq <sub>3</sub> phen <sub>3</sub>
Tb-N	499.0	497.0
Tb-O	578.0	564.0
Aromatic ring	736.0	735.0
	802.0	797.0
	835.0	834.0
	1319.0	1317.0
C-N	1395.0	1386.0
C=C	1508.0	1493.0
C-H	1028.0	1030.0
C=N	1577.0	1575.0
	1609.0	1600.0
C-O	1113.0	1111.0

The similar characteristics detected in the spectra indicate that all the Tbq<sub>3</sub> ternary complexes were of similar structure. This is due to the fact that all the ligands that are involved in the complexation are constructed from pyridine and phenol ring. It should be noted that the differences in intensities of particular bonding are associated to the addition of the neutral ligand that were involved in the coordination. This can be explained as, upon the coordination of the neutral ligand, the number of the nitrogen atom attached to the complexes is increased, thereby enhanced the electronegativity value of the complexes and as well as the bond dipole which consequently will result an intense absorption band.

### 4.3. X-Ray diffraction analysis

#### 4.3.1. $\text{Euq}_3\text{bpy}_3$ and $\text{Euq}_3\text{phen}_3$

Figure 4.3 shows the XRD spectra of  $\text{Euq}_3\text{bpy}_3$  and  $\text{Euq}_3\text{phen}_3$  thin films. From the spectra, it can be observed a broad diffraction hump located at around  $2\theta \approx 25^\circ$ . This verified that all the  $\text{Euq}_3$  ternary complexes are in the form of amorphous thin films. It is known that the amorphous films are held together by weak van der Waals interaction that couple the molecular orbitals of neighboring sites only weakly.

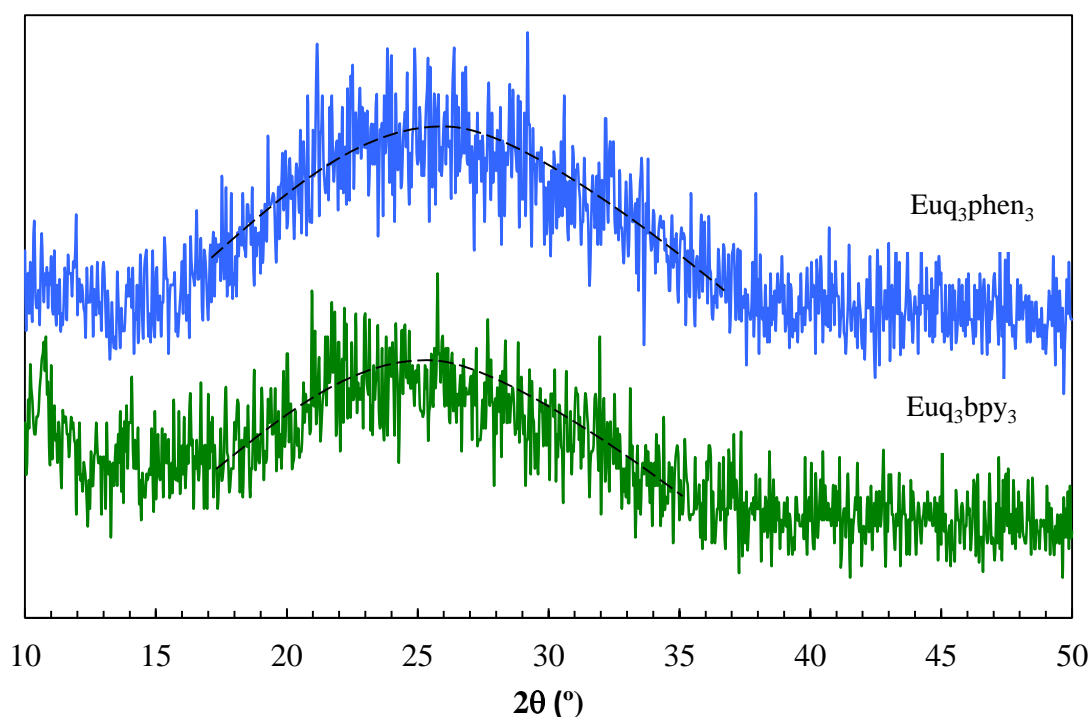


**Figure 4.3** X-ray diffraction (XRD) patterns of (a)  $\text{Euq}_3\text{bpy}_3$  and (b)  $\text{Euq}_3\text{phen}_3$

In particular, the weak intermolecular interaction that presence in amorphous films will result in localized molecular orbital, which is expected to have a smaller dielectric constant and thus reduced coulomb attraction (Kohler & Bassler, 2011). As a consequence, exciton generation is easily achieved and thereby enhanced the overall probability of radiative decay (Veinot & Marks, 2005). Therefore the



photoluminescence efficiency is expected to be high and thus offers a great potential for fabricating high luminescent properties OLED from this complex.

#### 4.3.2. $Tbq_3bpy_3$ and $Tbq_3phen_3$

Figure 4.4 shows the XRD spectra of  $Tbq_3bpy_3$  and  $Tbq_3phen_3$  thin films. It could be seen in the spectra that the entire  $Tbq_3$  ternary complexes exhibits a broad diffraction hump in the region of  $2\theta \approx 20^\circ$ - $30^\circ$  with a peak maximum at  $2\theta \approx 25^\circ$ . There was no significant crystalline peak observed indicating that these terbium complexes formed amorphous thin films.

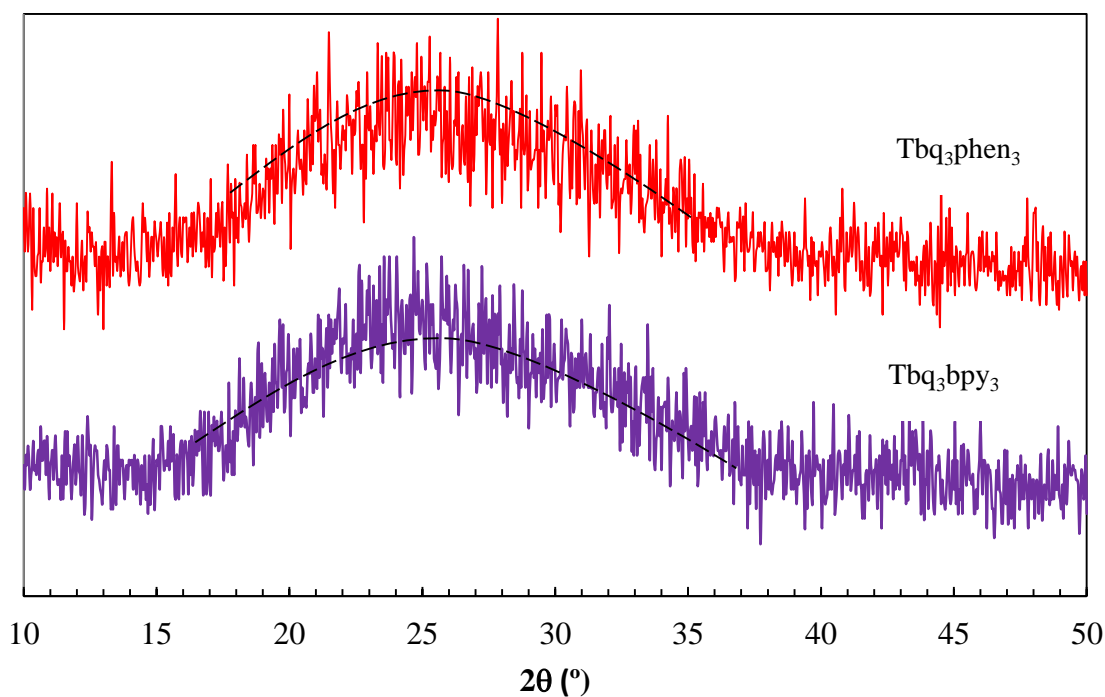


**Figure 4.4** X-ray diffraction (XRD) patterns of (a)  $Tbq_3bpy_3$  and (b)  $Tbq_3phen_3$

As mention in 4.3.1, a weak intermolecular interaction that governed in an amorphous thin film will result in localized molecular orbital which have consequence on dominance of exciton. Thus, photoluminescence efficiency of these complexes is also expected to be high with regard to the disorder structure of the thin film. Due to that

reason the photoluminescence efficiency is also expected to be high and thus can be categorized as potential rare earth complexes for OLED.

#### 4.4. DSC-TGA analysis

##### 4.4.1. *Euq<sub>3</sub>bpy<sub>3</sub>* and *Euq<sub>3</sub>phen<sub>3</sub>*

The stability and thermal decomposition pathway of Euq<sub>3</sub> ternary complexes were investigated by thermogravimetric analysis (TGA). The differential thermogravimetric (DTG) is the first derivatives of the TGA and is given as visual aid to distinguish between the overlapping weight loss step in TGA curve. It should be noted that DTG graph is exactly the same as the TGA except the weight loss versus time output is differentiated automatically to give the weight loss rate versus time. The peak temperature of maximum rate of weight loss, T<sub>DTG</sub> is obtained from the intersection of tangents to the peak of DTG curve. Figure 4.5 and 4.6 present the recorded TGA/DTG curves for two Euq<sub>3</sub> ternary complexes in nitrogen atmosphere at heating rate 20 °C/min. The characteristics parameters of the thermal decomposition are summarized in Table 4.3. Although these two metal complexes are identical in terms of the metal and the centre ligand (8Hq ligand) these curves, however show clear difference in thermal decomposition behavior.

The TGA/DTG curves for Euq<sub>3</sub>bpy<sub>3</sub> complex shows six decomposition steps in the range of 34- 893 °C (Figure 4.5). The TGA curve shows a weight loss of 0.47% in the range of 34-101 °C with a weak T<sub>DTG</sub> peak at 90 °C that was assigned to the loss of water molecule in the coordination sphere. It should be noted that the removal of the water molecule has occur below 100 °C. This is most likely due to the fact that the weight loss process has not been completed before the next step start. The second step shows a broad decomposition feature at the 100- 234 °C range with T<sub>DTG</sub> at 190 °C. At

this step, the DTG curve displays a broad decomposition features with a weight loss of 10.04% suggesting partial elimination of the Bpy ligand. The third steps that occur over the small temperature range (233- 297 °C) clearly show a small decomposition features with a weak  $T_{DTG}$  at 250 °C is followed by a weight loss of 4.15%. This weight loss is attributed to the elimination of the remaining Bpy ligand. As the temperature increased in the 296- 426 °C range, a weight loss of 8.10% with a sharp peak  $T_{DTG}$  at 380 °C indicate a rapid decomposition of 8Hq ligand. The following steps (step five and six) of decomposition exhibits a progressive weight loss within range 425- 893 °C may correspond to the partial decomposition of the remaining ligand molecules. The total weight loss up to 890 °C leaves 66.65% residual weight indicates that the decomposition of the remaining compound could not be completed even at 900 °C.

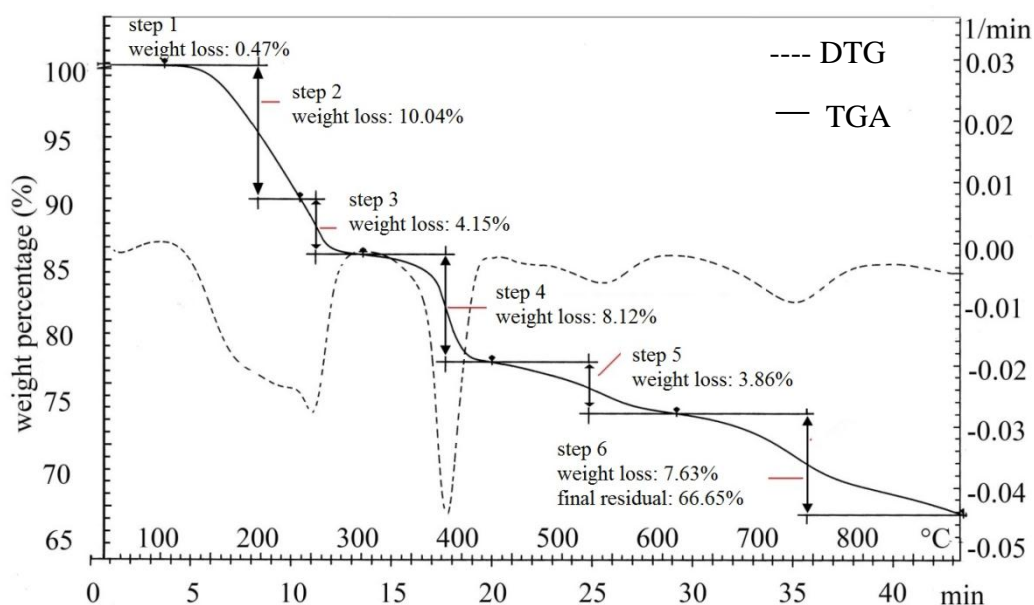


**Figure 4.5** TGA and DTA traces of Eu<sub>3</sub>bpy<sub>3</sub>

A rather different thermal behavior was shown by Eu<sub>3</sub>phen<sub>3</sub> complex (Figure 4.6). From the TGA/DTG curve, it is noticeable that only two remarkable decomposition steps were involve within the range of 35-893 °C. The complex is stable up to 260 °C after which it starts drastically decompose within the temperature range 34- 331 °C. A

weight loss of 24.97% with strong  $T_{DTG}$  310 °C is corresponded to the partial decomposition of the 8Hq ligand. The second decomposition step occurs in the range of 330- 893 °C. At this step, the DTG curve yields the maximum decomposition rates of  $T_{DTG}$  340 °C with a weight loss of 29.62% that is associated to the elimination of the remaining 8Hq ligand. Finally a 45.40% residual was obtained.

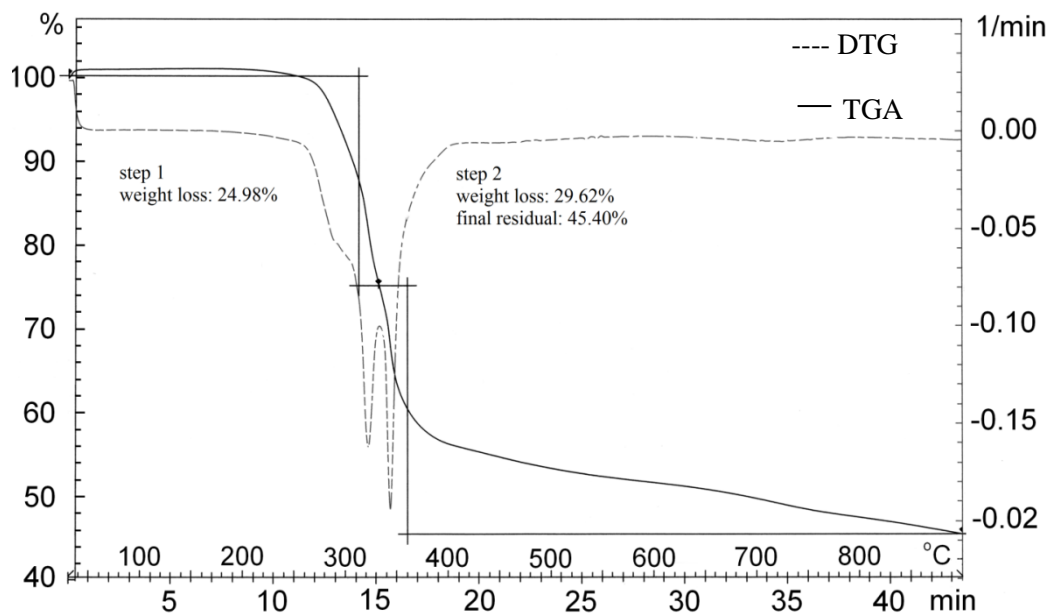


Figure 4.6 TGA and DTG traces of  $\text{Euq}_3\text{phen}_3$

Table 4.3 Characteristics parameters of thermal decomposition for  $\text{Euq}_3\text{bpy}_3$  and  $\text{Euq}_3\text{phen}_3$  complexes

Complex	Step	Temperature range	% weight loss found	DTG peak temperature	Final residue weight found (%)
$\text{Euq}_3\text{bpy}_3$	1	34-101	0.47	90	66.65
	2	101-234	10.04	190	
	3	234-297	4.15	250	
	4	297-426	8.10	380	
	5	426-609	3.88	525	
	6	609-893	7.63	740	
$\text{Euq}_3\text{phen}_3$	1	35-331	24.98	310	45.40
	2	331-893	29.62	361	

#### 4.4.2. $Tbq_3bpy_3$ and $Tbq_3phen_3$

The thermogravimetric (TGA) and differential thermogravimetric (DTG) analysis which characterized the thermal decomposition of  $Tbq_3$  ternary complexes in nitrogen atmosphere at heating rate 20 °C/min are given in Figure 4.7 and 4.8. It should be noted that DTG graph is exactly the same as the TGA except that the weight loss versus time output is differentiated automatically to give the weight loss rate versus time. The peak temperature of maximum rate of weight loss,  $T_{DTG}$  is obtained from the intersection of tangents to the peak of DTG curve. The important characteristics of thermal decomposition parameters are summarized in Table 4.4. As mentioned in section 4.4.1 the TGA/DTG curves of the  $Tbq_3$  ternary complexes are also found to exhibit different thermal decomposition behavior despite of similar rare-earth metal and the centre ligand (8Hq ligand).

From Figure 4.7, it could be seen that  $Tbq_3bpy_3$  complex shows six decomposition steps in the range of 34- 893 °C. The first decomposition steps detected in the TGA curves of  $Tbq_3bpy_3$  complex at the 34-89 °C range with their  $T_{DTG}$  in DTG curves at 70 °C shows weight loss of 0.72% is corresponded to the presence of the water molecule in the coordination sphere. The second steps of  $Tbq_3bpy_3$  complex shows a slow decomposition feature in the 88- 157 °C range with a weak and small  $T_{DTG}$  at 140 °C. At this step, the DTG curve displays a weight loss of 2.3% weight suggesting an extremely slow elimination of the Bpy ligand. The third steps of  $Tbq_3bpy_3$  complex in the 156-332 °C range clearly shows a rapid decomposition features with a large and strong  $T_{DTG}$  at 250 °C is followed by a weight loss of 20.00%. This weight loss is attributed to the elimination of the remaining Bpy ligand. The fourth steps (331- 456 °C) with a broad and small peak  $T_{DTG}$  395 °C indicates that the weight loss of 5.0% is due to the degradation of 8Hq ligand.

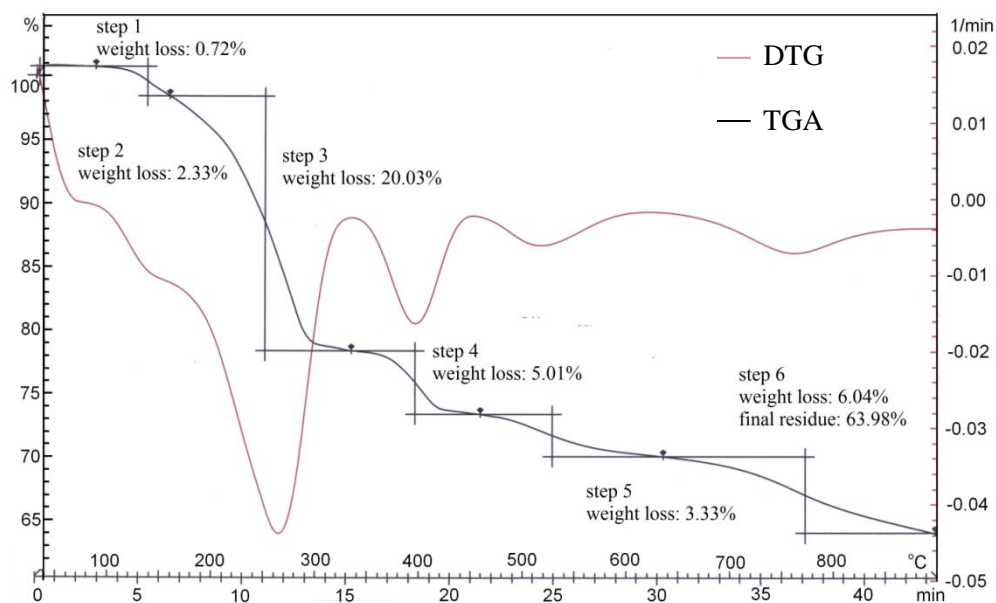


Figure 4.7 TGA and DTG traces of  $Tbq_3bpy_3$

The remaining steps (step five and six) of decomposition occur within a range of 455-890 °C may correspond to the partial decomposition of the remaining ligand molecules. The total weight loss up to 890 °C leaves 63.98% residual weight indicates that the decomposition of the remaining compound could not be completed even at 900 °C.

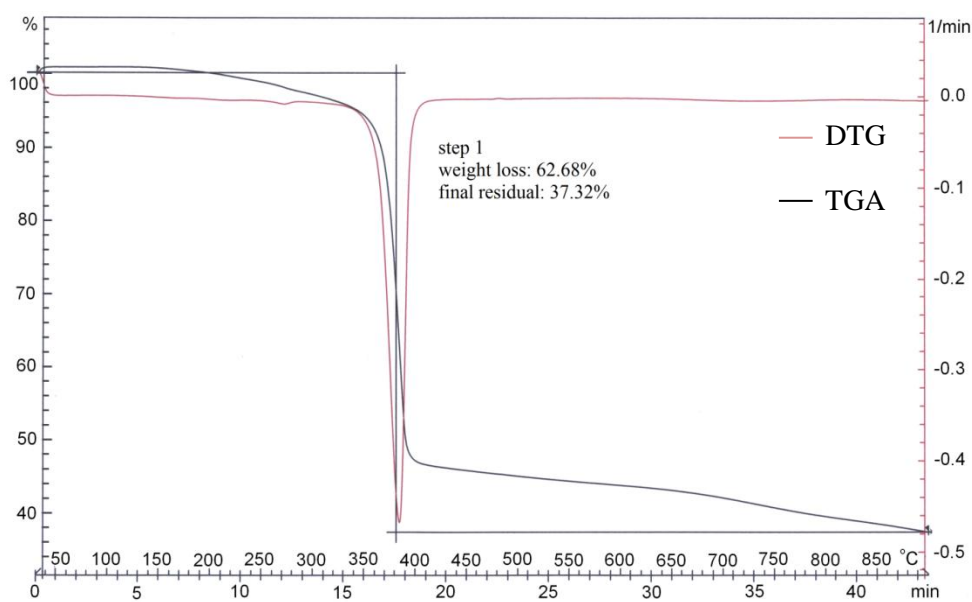


Figure 4.8 TGA and DTG traces of  $Tbq_3phen_3$

Figure 4.8 shows the decomposition pathway for  $Tbq_3phen_3$  complex. Unlike the other complexes,  $Tbq_3phen_3$  complex shows only one step obvious decomposition. The process of decomposition is more rapid compare to the other complexes. The TGA curve shows that the complex is stable up to 350 °C after which it starts drastically decompose within the temperature range 34- 893 °C. The weight loss of 62.8% with a large and strongly sharp peak  $T_{DTG}$  at 390 °C indicating a progressive weight loss process which leaves 37.72% residual.

**Table 4.4 Characteristics parameters of thermal decomposition for  $Tbq_3bpy_3$  and  $Tbq_3phen_3$  complexes**

Complex	Step	Temperature range (°C)	% weight loss found	DTG peak temperature	Final residue weight found (%)
$Tbq_3bpy_3$	1	35-89	0.47	70	63.98
	2	89-157	10.04	140	
	3	157-332	4.15	250	
	4	332-456	8.10	395	
	5	456-632	3.88	525	
	6	632-891	7.63	770	
$Tbq_3phen_3$	1	35-893	34.07	390	37.32

#### 4.5. Conclusion

The IR spectra of the  $Euq_3$  ternary complexes indicate that the complexes were of similar structure. Similar results are found from FTIR spectra of  $Tbq_3$  ternary complexes. Some slight shifts and intensity changes can be related to the different type of neutral ligand in the ternary complexes. XRD spectra of the thin films of the complexes show that their structures are amorphous and thus it can be expected that the thin films of the complexes can produce high photoluminescence efficiency. It also can be seen that even though the  $Euq_3$  and  $Tbq_3$  ternary complexes are identical in terms metal centre and centre ligand (8Hq ligand), their thermal decomposition behavior are not the same and depends on the neutral ligand attach to the complexes.